Desalination and Water Treatment
www.deswater.com

doi: 10.5004/dwt.2020.25028

179 (2020) 148–159
March

Optimization of the conditions for degradation of hydrolyzed polyacrylamide using electro-coagulation

Sitao Zhang[a,b,c], Yanhe Han[b,*], Xiaofei Zhang[a], Chuantao Wu[b], Ran An[b]

[a]*State Key Laboratory of Petroleum Pollution Control, CNPC Research Institute of Safety and Environmental Technology, Beijing 102206, China, emails: 1106694473@qq.com (S. Zhang), xiaofei_zhang@126.com (X. Zhang)*
[b]*Department of Environmental Engineering, Beijing Institute of Petrochemical Technology, Beijing 102617, China, emails: hanyanhe@bipt.edu.cn (Y. Han), 1218008836@qq.com (C. Wu), 18811103086@qq.com (R. An)*
[c]*Beijing University of Technology, Beijing 100124, China*

Received 23 May 2019; Accepted 14 October 2019

ABSTRACT

The wastewater produced during tertiary oil recovery often contains a large amount of hydrolyzed polyacrylamide (HPAM), which is difficult to treat using conventional biological methods because of its high molecular weight and viscosity. Electrochemical methods are considered to be effective for the treatment of refractory wastewater. In this study, the electrochemical degradation of HPAM using several anode materials was investigated. The results show that the highest HPAM removal efficiency was obtained when iron was used as the anode. The effects of the reaction time, voltage, current density, electrode distance, initial pH, and temperature on the efficiency of HPAM removal were investigated using single-factor experiments, and the HPAM removal rate was found to depend most strongly on the reaction time, voltage, and initial pH. Based on these results, Box–Behnken design was used to optimize the electrochemical treatment of HPAM, and the optimal conditions for HPAM removal were determined to be the following: voltage = 7.6 V, pH = 4.7, and reaction time = 10.5 min. The optimal conditions were tested experimentally, and the HPAM removal efficiency was found to be 98.4%, which fell within the 95% confidence interval of the model results. Analysis of the degradation mechanism showed that HPAM removal occurred mainly via electro-coagulation, with a contribution rate of 83%, together with electro-oxidation, and that the degradation intermediates included ammonia and ethers. Therefore, this electrochemical technique is effective for treatment of wastewater containing HPAM.

Keywords: Iron anode; Response surface methodology (RSM); HPAM; Electro-coagulation

1. Introduction

Petroleum is a major energy resource worldwide. To enhance oil recovery, hydrolyzed polyacrylamide (HPAM) is widely used in the oil industry. Because HPAM is water-soluble, large volumes of wastewater containing HPAM are discharged into the environment [1]. Although HPAM itself is not toxic, it is easily degraded into intermediate products that are harmful to the environment and human health. Hence, HPAM should be removed from wastewater before it is discharged into the environment [2].

Many HPAM degradation methods have been applied to wastewater in China and other countries, including physical [3], chemical oxidation [4], and biological methods [5]. Among them, biological treatment is usually considered to be economic and efficient for wastewater treatment. However, biological treatment of HPAM-containing wastewater is difficult. Therefore, biological methods are generally combined with a physical or chemical method to treat

* Corresponding author.

HPAM-containing wastewater. Pi et al. [2] used a combination of Fenton oxidation and an anaerobic biological process to treat HPAM and achieved an HPAM removal rate of 91.06%. However, the processing time was longer than 40 d, an extended operating period was required, and the economic efficiency of the process was low.

Electrochemical treatment represents a promising physicochemical technology for the removal of various pollutants [6]. Electrochemical methods have many advantages. They can utilize simple device structures, are easy to operate, and require short processing times; additionally, the raw materials used for the electrodes are abundant, and their reaction products are environmentally friendly. Electrochemical methods, particularly electro-coagulation (EC) and electro-oxidation (EO), have been studied for the treatment of various types of refractory industrial wastewater [7,8]. In EC, a metal hydroxide colloid produced by the electrode removes contaminants from the wastewater via adsorption bridging and coprecipitation. The electrode reactions are given in Eqs. (1)–(5) [9]:

$$Fe \rightarrow Fe^{2+} + 2e^- \quad (1)$$

$$2H_2O + 2e^- \rightarrow 2OH^- + H_2 \quad (2)$$

$$Fe^{2+} + 2OH^- \rightarrow Fe(OH)_2 \quad (3)$$

$$4Fe(OH)_2 + O_2 + 2H_2O \rightarrow 4Fe(OH)_3 \quad (4)$$

$$nFe(OH)_3 \rightarrow Fe(OH)_{3n} \quad (5)$$

In EO, pollutants are degraded by strong oxidants, such as active chlorine and hydroxyl radicals. The reactions are shown in Eqs. (6)–(8) [10]:

$$2Cl^- - 2e^- \rightarrow Cl_2 \quad (6)$$

$$Cl_2 + H_2O \rightarrow HClO + H^+ + Cl^- \quad (7)$$

$$MO_X + H_2O \rightarrow MO_X(^{\bullet}OH) + H^+ + e^- \quad (8)$$

The mechanism and efficiency of the oxidation of organic substances depends on the electrode materials. Graphite is a very cheap and abundant electrode material, and exhibits both EO and adsorption mechanisms for pollutant removal due to its large surface area. Platinum is a stable and relatively available electrode material that is usually used to treat dye wastewater. However; these two electrodes have low oxygen evolution overpotentials and low pollutant degradation efficiencies. Boron-doped diamond (BDD) and dimensionally stable anodes have high oxygen evolution overpotentials, which allows them to effectively degrade organic pollutants [11].

There have been few studies on the treatment of HPAM-containing wastewater using electrochemical methods. Zhu et al. [3] used aluminum sheets as working electrodes to treat HPAM-containing wastewater and obtained good experimental results. However, their discussion of experimental optimization and the electrochemical degradation of HPAM was inadequate. In addition, the treated solution contained aluminum, which is harmful to human health and is believed to cause Alzheimer's disease [12]. Moreover, the aluminum anode had a low chemical oxygen demand removal efficiency for wastewater and a high energy requirement, resulting in high operation costs [13,14]. Therefore, an efficient, nontoxic anode for the degradation of HPAM should be identified. To this end, further exploration of the optimal electrode materials and experimental conditions, as well as the underlying mechanism of degradation, is needed.

The response surface method can be used to evaluate the interaction between different independent variables and effectively reduce the number of experiments required for optimization [15]. Box–Behnken design (BBD) is one model of the response surface method, and is based on a three-level design and a fitted second-order response surface. In the optimization experiments, each factor is relevant with a 2^2 factorial and the replicate number of the central point. The number of experiments (n) depends on the expression $n = 2^2 \times k \times (k–1)/2 + C_0$, where k is the number of variables and C_0 is the replicate number of the central point [16,17].

In this study, the electrochemical degradation of HPAM was investigated using three anode materials: BDD, iridium–ruthenium–titanium (Ir–Ru–Ti), and an iron plate. The effects of the reaction time, voltage, current density, electrode distance, initial pH, and temperature on the efficiency of HPAM treatment using the optimal electrode were investigated in single-factor experiments. To optimize the experimental conditions, the three main factors influencing the degradation efficiency were identified based on the single-factor experiment results and then optimized using BBD. The HPAM degradation mechanism was also investigated. The results provide useful information for the design of an electrochemical unit to degrade HPAM-containing wastewater.

2. Methodology

2.1. Materials and reagents

The HPAM, hydrochloric acid, acetic acid, soluble starch, bromine water, sodium formate, sodium acetate, cadmium iodide, sodium chloride, and aluminum sulfate used in the study were all of analytical reagent grade (Ketuo Chemical, Beijing, China). Ir–Ru–Ti electrodes and iron plates were purchased from Baoji Changli Special Metal Co. Ltd. A BDD electrode was purchased from Adamant Technologies (Switzerland). All the anodes used in this study had dimensions of 30 mm × 60 mm × 1 mm, and were immersed in the solution to a depth of 40 mm.

2.2. Preparation of the samples and electrodes

The HPAM used in the experiment had a molecular weight of 3×10^6 and a degree of hydrolysis of 10%. The simulated wastewater contained 200 mg L^{-1} of HPAM and 6 g L^{-1} of NaCl.

The Ir–Ru–Ti electrodes were immersed in a 10% NaOH solution for 30 min to remove surface grease and then washed repeatedly with deionized water.

The BDD electrodes were placed in an alcohol solution, ultrasonically cleaned for 5 min to remove surface impurities, and then rinsed repeatedly with deionized water.

The iron plates were first ground with 1200 P sandpaper and soaked in 10 wt% NaOH for 30 min to remove surface oil. They were subsequently rinsed with deionized water, soaked in 10 wt% HCl for 15 min, and then rinsed again with deionized water.

2.3. Electrochemical experiments and analytical methods

The experiments were conducted in 100 mL custom-built Plexiglass reaction vessels. The actual reaction volume was 80 mL. The anode materials were iron plate, Ir–Ru–Ti, and BDD. The cathodes were sheets of 304 stainless steel with dimensions of 30 mm × 60 mm × 1 mm. A magnetic stirrer (DF-101S, Yushen, China) was used for continuous stirring during the reaction.

The initial pH was adjusted using 0.1 mol L^{-1} HCl or NaOH and measured using a digital pH meter. The voltage was controlled by a precision digital direct power supply (0–5 A, 0–30 V, CSI12005S DC power supply), and the temperature was controlled by a water bath. All products were collected after being allowed to precipitate for 30 min after the end of the reaction. A UV spectrophotometer (Model UV-2600, SHIMADZU, Japan) operating at 585 nm was used to measure the HPAM concentration via the starch–cadmium–iodine method [18]. The HPAM removal rate was calculated using Eq. (9) below:

$$\text{HPAM removal rate}(\%) = \frac{C_0 - C_t}{C_0} \times 100\% \tag{9}$$

where C_0 (mg L^{-1}) is the initial concentration of HPAM, and C_t (mg L^{-1}) is the final concentration of HPAM.

After the reaction, the precipitate was concentrated using a centrifugal separator (TG16-WS, Cence, China). The concentrated precipitate was placed in a beaker, diluted to 80 mL with deionized water, adjusted to pH = 3 with hydrochloric acid, and stirred for 12 h with a force stirrer until the precipitate was completely dissolved. The HPAM concentration was subsequently measured, and the amount of HPAM removed was calculated. The ammonium nitrogen in the solution after the degradation reaction was detected using an ammonia nitrogen analyzer (PCOD-810, Changhong, China).

The HPAM in the precipitate after the degradation reaction was qualitatively analyzed using Fourier transform infrared (FT-IR) spectrometry (Tensor 27, Bruker, Germany). For comparison, FT-IR spectra of the flocs produced by electrolysis of a pure NaCl solution and of pure HPAM were also obtained. All the samples were dried in an oven at 50°C.

To investigate the contribution of EC, the amount of HPAM in the floc solid was measured. The measurement was carried out using the method published by Ahmadi et al. [19]. Simply, the filtered precipitate from the experiment with coagulated HPAM was washed three times with deionized water and dried at 70°C until a constant weight was achieved, after which the HPAM content was determined.

2.4. Experimental design

2.4.1. Single-factor experiments

The single-factor experiments investigated the effects of the reaction time, voltage, current density, electrode distance, initial pH, and temperature on the HPAM removal rate. We identified the three factors that had the greatest impact on the HPAM removal rate and subsequently explored their optimal ranges.

2.4.2. Response surface method experimental design

The experiment was designed using the Box–Behnken method in the software package Design Expert (Design Expert 8.0.6). Based on the results of the preliminary experiments, the voltage (X_1), initial pH (X_2), and reaction time (X_3) were selected as the three main factors for the response surface methodology (RSM). Values of –1, 0, and 1 were used to indicate low, intermediate, and high levels, respectively, as shown in Table 1.

The second-order model and optimal experimental conditions from the response values and factors were analyzed using the RSM, as shown in Eq. (10) [15]:

$$Y = a_0 + \sum_{i=1}^{k} a_i X_i + \sum_{i=1}^{k} a_{ii} X_i^2 + \sum_{1 \le i \le j}^{k} a_{ij} X_i X_j + \varepsilon \tag{10}$$

where Y represents the HPAM removal rate; a_0 is a constant term (intercept); X_i and X_j are variables; a_i, a_{ii}, and a_{ij} are the primary, quadratic, and interaction coefficients, respectively; and ε indicates the experimental residual.

3. Results and discussion

3.1. Electrode selection

To investigate the removal of HPAM by EC and EO, iron plate was selected as a typical representative electrode for EC, and BDD and Ru–Ir–Ti electrodes were selected as typical EO electrodes in this study. The HPAM solution was treated using a constant voltage of 5 V, an electrode distance of 2 cm, a reaction time of 30 min, an initial pH of 6.5, and an initial temperature of 25°C, respectively. The experimental results are shown in Fig. 1.

As shown in Fig. 1a, the HPAM removal rate using the iron electrode was 92.5%, which was significantly higher than that obtained using the other electrodes. This result was similar to that reported by Wang and Wang [20]. Iron anodes are generally considered to be efficient for EC. The iron ions

Table 1
Box–Behnken experimental design factor levels

Level	Factors		
	Voltage (V, X_1)	Initial pH (X_2)	Reaction time (min, X_3)
Low level (–1)	1	4	5
Intermediate level (0)	5	8	10
High level (+1)	9	12	15

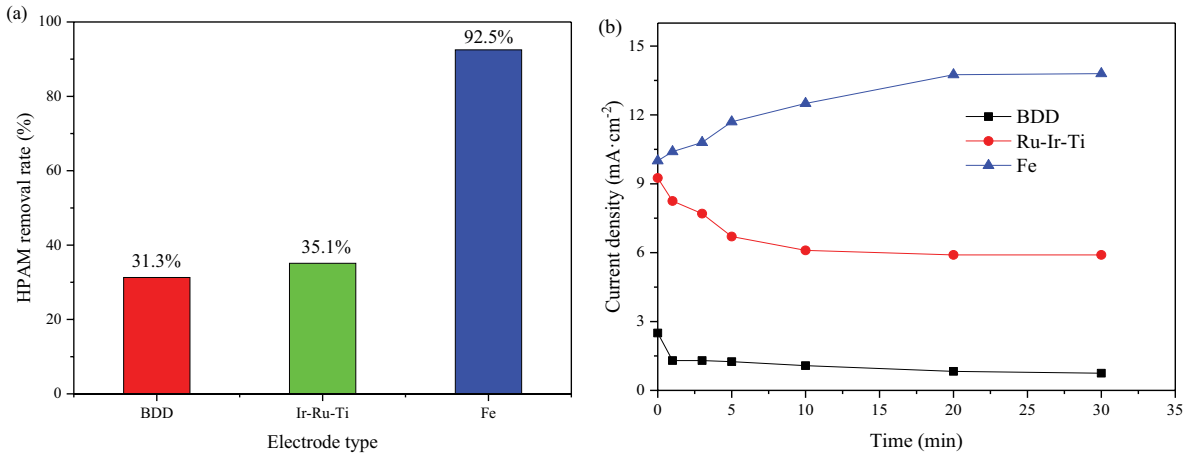

Fig. 1. HPAM removal efficiencies (a) and current densities (b) of the different electrodes (constant voltage: 5 V, electrode distance: 2 cm, reaction time: 30 min, initial pH: 6.5, temperature: 25°C).

released from the anode can easily form $Fe(OH)_2/Fe(OH)_3$ flocs, which can effectively remove pollutants from the wastewater. Considering the characteristics of HPAM and the iron flocs, the removal of HPAM is believed to take place predominantly via polymer-bridging, charge patch attraction, complex formation, and depletion flocculation mechanisms [21]. As shown in Fig. 1a, the BDD and Ru–Ir–Ti electrodes, which were used as EO electrodes, exhibited lower HPAM removal rates. This indicated that EC was more efficient than EO for the removal of HPAM under the experimental conditions. However, the HPAM-containing sludge generated by EC requires further treatment. Fig. 1b shows the current densities obtained using the different electrodes at a constant voltage of 5 V. The Fe electrode exhibited the highest current density at this voltage, which was consistent with the HPAM removal results. The removal efficiency of HPAM was consistent with the relative magnitudes of current density at a reaction time of 30 min. Therefore, Fe was selected as the optimal anode for the removal of HPAM.

3.2. Effect of the reaction time

Reaction time has a critical impact on electrochemical reactions. Shorter reaction times usually result in incomplete removal of contaminants, whereas longer times cause excessive energy loss at the electrode [22]. Different pollutants require different reaction times. Therefore, the effect of reaction time (0–30 min) on HPAM removal under magnetic stirring was investigated using a voltage of 5 V, an electrode distance of 2 cm, an initial pH of 6.5, and an initial temperature of 25°C.

As shown in Fig. 2a, the HPAM concentration generally decreased with time. During the first 2 min, the HPAM concentration changed little, and the degradation rate was very low (only 1.7%). The low degradation rate was probably due to only a small amount of Fe^{2+} having been dissolved at the anode, resulting in insufficient formation of the flocs that were responsible for settling of contaminants. As the reaction time was increased from 2 to 10 min, the HPAM removal efficiency increased from 1.7% to 91.8%. In theory,

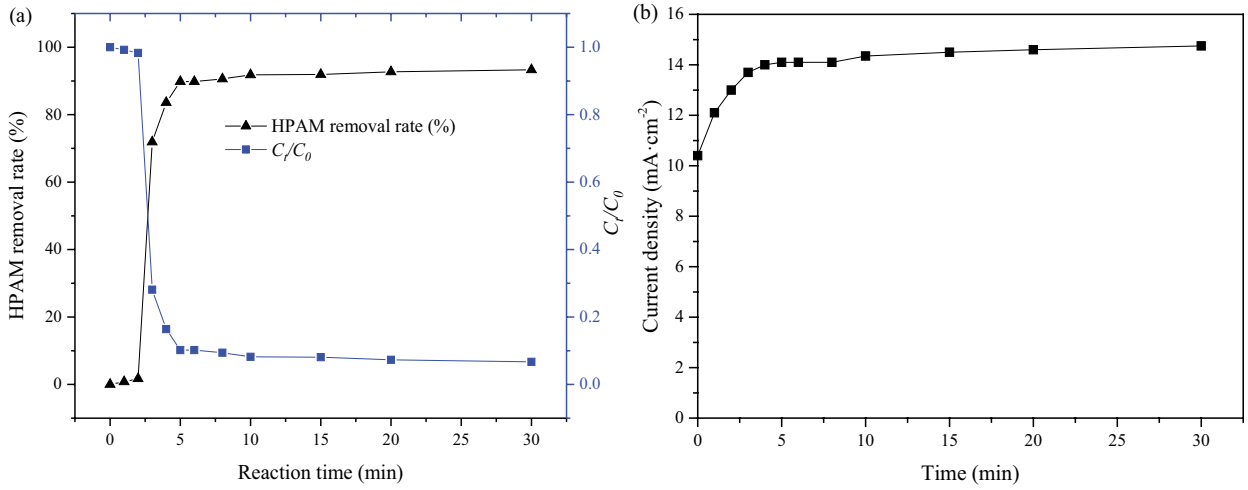

Fig. 2. Effect of the reaction time on the HPAM removal rate (a), and the variation of the current density with reaction time (b) using an iron electrode (constant voltage: 5 V, electrode distance: 2 cm, initial pH: 6.5, temperature: 25°C).

this may have been related to an increase in the amount of Fe^{2+} and the generation of nascent flocs [23,24]. The HPAM degradation rate reached a peak at approximately 10 min, after which it became constant, and no obvious change was observed. This might have been related to the saturation of floc adsorption in the solution [25]. The dissolved Fe^{2+} increased the current density, and the current density trend was consistent with that of the HPAM removal efficiency. The current density tended to become stable at about 10 min, as shown in Fig. 2b.

When the reaction time exceeded 10 min, the amount of electrochemical sludge generated by the reaction system also increased greatly, making sludge disposal more difficult in the later stages. Therefore, the optimal experimental reaction time was determined to be 10 min.

3.3. Effect of the voltage

The magnitude of the voltage directly determines whether an electrochemical reaction can occur, controls the reaction rate, and affects the growth of flocs; thus, it is a highly significant parameter in electrochemical reactions [26]. The variable voltage experiment was conducted at an initial pH of 6.5, an initial temperature of 25°C, an electrode distance of 2 cm, and a reaction time of 10 min under magnetic stirring. The voltage was varied from 1 to 9 V. The result is shown in Fig. 3a.

Fig. 3a shows that the HPAM removal rate was very low (5.5%) at 1 V. This was attributed mainly to the very low quantity of Fe^{2+} dissolved at the anode and the negligible amount of EC at this voltage. Under these conditions, HPAM was degraded mainly through EO via hydroxyl radicals and active chlorine.

As the voltage was increased from 1 to 9 V, the HPAM removal efficiency increased from 5.5% to 92.8% due to the increased number of electrons and Fe^{2+} ions, which in turn increased the number of flocs, thereby enhancing the contaminant removal [27]. The current density also increased as the voltage was increased, as shown in Fig. 3b. Additionally, metal hydroxide neutralizes static charges dispersed on the contaminant particles, reduces the electrostatic repulsion between particles, and increases the van der Waals force between particles, thereby promoting particle aggregation [28].

Moreover, the HPAM removal rate increased significantly when the voltage was increased from 1 to 2 V. As the voltage was further raised from 2 to 5 V, the HPAM removal rate also increased gradually. However, when the voltage exceeded 5 V, the HPAM removal rate tended to plateau. Although the energy consumption increased when the voltage was increased from 2 to 5 V, 5 V was selected as the working voltage in the following experiment in order to ensure the effective removal of HPAM.

3.4. Effect of the current density

Like voltage, current density also has a strong effect on electrochemical degradation processes. The effect of current density was experimentally investigated at an initial pH of 6.5, initial temperature of 25°C, an electrode distance of 2 cm, and a reaction time of 10 min under magnetic stirring. The current density was varied from 1 to 20 mA cm^{-2}; the results are shown in Fig. 4.

The effect of the current density was similar to that of the voltage. The HPAM removal rate increased with increasing current density, as shown in Fig. 4a. At the lowest current density tested (1 mA cm^{-2}), the HPAM removal rate was 36.5%. However, at current densities of 5 and 10 mA/cm^2, the HPAM removal rates were 91.5% and 91.7%, respectively. This can be attributed to two phenomena. First, as the current density was increased, the amount of Fe^{2+} produced also increased; this was favorable for the formation of $Fe(OH)_2$/$Fe(OH)_3$, which enhanced the flocculation of HPAM. Second, the increase in current density may have increased the amount of strongly oxidizing substances such as HClO and OH, which may have contributed to the increase in the HPAM removal rate [29]. Although both voltage and current density had similar trends with regards to the removal rate, the HPAM removal rate more likely depends on the voltage, because the redox potential is a controlling factor at a

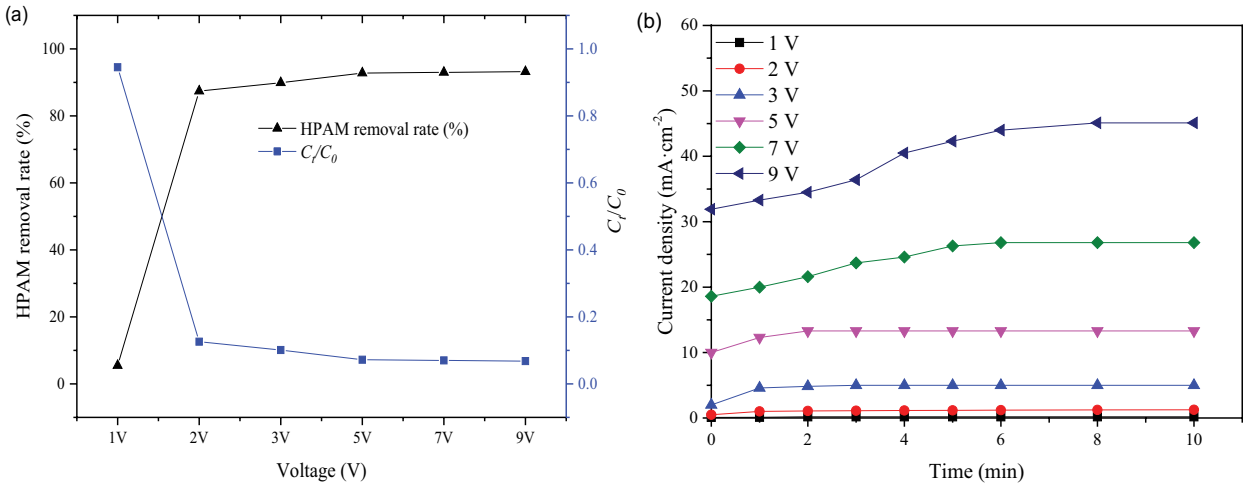

Fig 3. Effect of voltage on the HPAM removal rate using a reaction time of 10 min (a), and the resulting variation in the current density (b) at an iron electrode (electrode distance: 2 cm, initial pH: 6.5, temperature: 25°C, reaction time: 10 min).

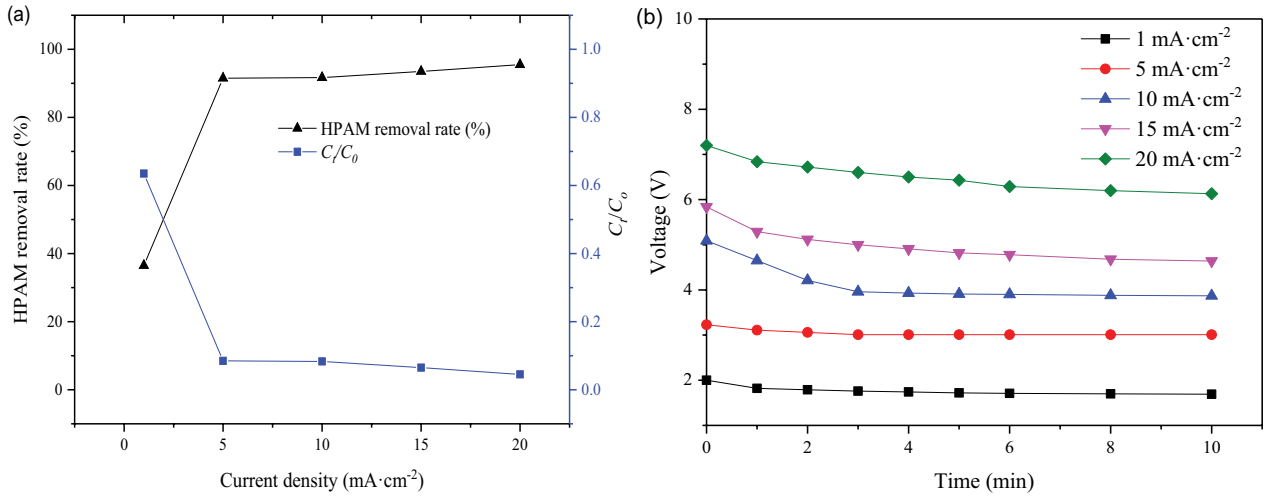

Fig. 4. HPAM removal rates at different constant current densities for a reaction time of 10 min (a), and corresponding variation of the voltage (b) at the iron electrode for different current densities (electrode distance: 2 cm, initial pH: 6.5, temperature: 25°C, reaction time: 10 min).

high electrolyte concentration [26]. Therefore, voltage was selected as the main factor in the follow-up experiment. The variation in the voltage at different constant current densities is shown in Fig. 4b.

3.5. Effect of the electrode distance

Electrode distance is an important parameter in electrochemical reactor design and strongly affects the current line distribution. The resistance of the solution typically increases as the electrode distance is increased. Additionally, the electric field lines become more dispersed, and the electric field strength decreases; consequently, the capacity for electrochemical treatment of pollutants is reduced. The electrode distance also determines the operating cost. The variable electrode distance experiment was conducted using a voltage of 5 V, an initial temperature of 25°C and initial pH of 6.5, and a reaction time of 10 min under magnetic stirring. The electrode distance was varied from 0.5 to 4 cm, and the results are shown in Fig. 5.

As the electrode distance was decreased from 4 to 1 cm, the HPAM removal rate increased from 90% to 93.1%, as shown in Fig. 5a. This occurred because the current (as shown in Fig. 5b) and mass transfer efficiencies were higher at smaller electrode distances. Furthermore, more flocs could be produced in the solution [29]. However, when the electrode spacing was reduced to 0.5 cm, the removal rate of HPAM was only 83.2%. This could be attributed to the formation of turbulence and poor mass transfer in the reactor at shorter distances [30]. When the electrode distance is too short under high electrostatic attraction conditions, metal hydroxides collide with each other and decrease [22].

The HPAM removal rate was similar at electrode distances of 1 and 2 cm. However, the number of electrode

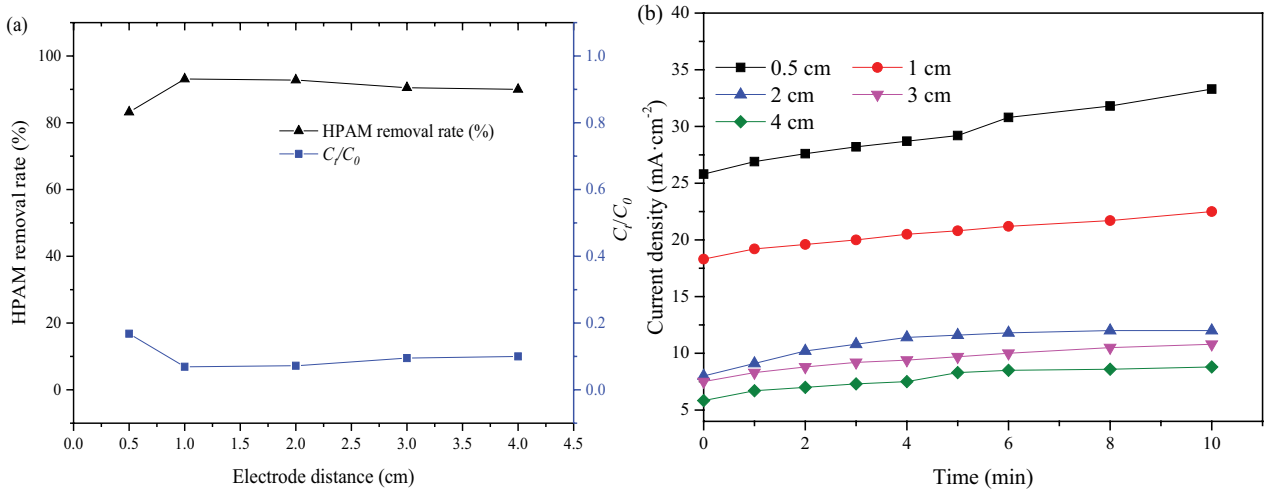

Fig. 5. Effect of the electrode distance on the HPAM removal rate for a reaction time of 10 min (a), and the corresponding variation of the current density (b) at an iron electrode (constant voltage: 5 V, initial pH: 6.5, temperature: 25°C, reaction time: 10 min).

plates was relatively low and less sludge was produced at a distance of 2 cm. Therefore, the optimal experimental electrode distance was determined to be 2 cm.

3.6. Effect of the initial pH

The initial pH is an important operating parameter that affects EC performance, as it influences the conductivity of the solution, zeta potential and electrode dissolution [31]. Therefore, the effect of pH during electrochemical treatment was investigated. The pH experiment was conducted at a voltage of 5 V, an electrode distance of 2 cm, an initial temperature of 25°C, and a reaction time of 10 min using a magnetic stirrer. The initial pH was varied from 2.0 to 12.0.

As shown in Fig. 6a, the HPAM removal rate was relatively high (greater than 85%) at pH values between 3 and 11. The current density is shown in Fig. 6b. The reason is that the Fe^{2+} and Fe^{3+} formed during the electrochemical reaction tend to form flocs composed of species such as $Fe(OH)_2$ and $Fe(OH)_3$ at pH = 3–11; these flocs exhibit strong adsorption of HPAM [32]. At high pH values (pH = 12), the degradation rate of HPAM was only 28.7%. This is because at highly alkaline pH values, the undesirable monomeric species $Fe(OH)_4^-$ is formed, and the amorphous $Fe(OH)_3$ flocs become fluffy and dissolve [13]. At low pH (pH = 2), the HPAM degradation rate was 66.1%. The OH^- ions were neutralized by the H^+ ions in the solution, and the cathode reduced the $Fe(OH)_3$ colloids. Therefore, the flocculation effect also decreased [33]. The degradation mechanism depends mainly on the strong oxidizing action of Fe^{3+} under acidic conditions. The highest HPAM removal rate (93.9%) was obtained at pH = 8. Therefore, the optimal experimental pH was determined to be 8.

3.7. Effect of the temperature

Temperature is a factor that is often ignored. Raising the temperature generally promotes mass transfer in the solution, which increases the reaction rate. The variable temperature experiment was conducted at a voltage of 5 V, an electrode distance of 2 cm, an initial pH of 8, and a reaction time of 10 min using a magnetic stirrer. The initial temperature was adjusted from 15°C to 45°C.

Fig. 7a shows that the degradation rate increased from 90% to 93.9% as the temperature was increased from 15°C to 45°C. The current density is shown in Fig. 7b. The increased degradation was possibly due to the increased ion and polymer mobility and collision rates with increasing temperature [34]. However, the trend was quite subtle. Thus, among the various factors tested, the temperature was found to have an insignificant impact on the HPAM degradation efficiency.

3.8. Response surface analysis

3.8.1. Establishment of the model and analysis of variance

The software Design-Expert (8.0.6) was used to analyze the experimental data. The experimental scheme and results are shown in Table 2.

Table 3 shows the results of the analysis of variance (ANOVA) of the experimental data. The ANOVA results for the three single factors (voltage, pH, and reaction time) were fitted to the polymer removal rate, and yielded the following quadratic polynomial (Eq. (11)):

$$Y = 86.22 + 35.77X_1 - 12.32X_2 + 8.7X_3 - 7.94X_1X_2 + 1.5X_1X_3 + 10.95X_2X_3 - 35.52X_1^2 - 10.72X_2^2 - 6.7X_3^2 \quad (11)$$

Here, Y represents the degradation rate of HPAM; X_1, X_2, and X_3 represent the voltage, initial pH, and reaction time, respectively. According to the ANOVA results, all three factors had significant effects, and their degree of influence followed the order voltage > initial pH > reaction time. The results show that strict control of the voltage is required when an electrochemical apparatus is used to process HPAM, and is key to ensuring the effective removal of HPAM.

The p value of the model was less than 0.0001, suggesting that the equation reflected the relationship between the polymer removal rate and the single factors well [35]. The F value was 56.04, indicating that the model was significant, and

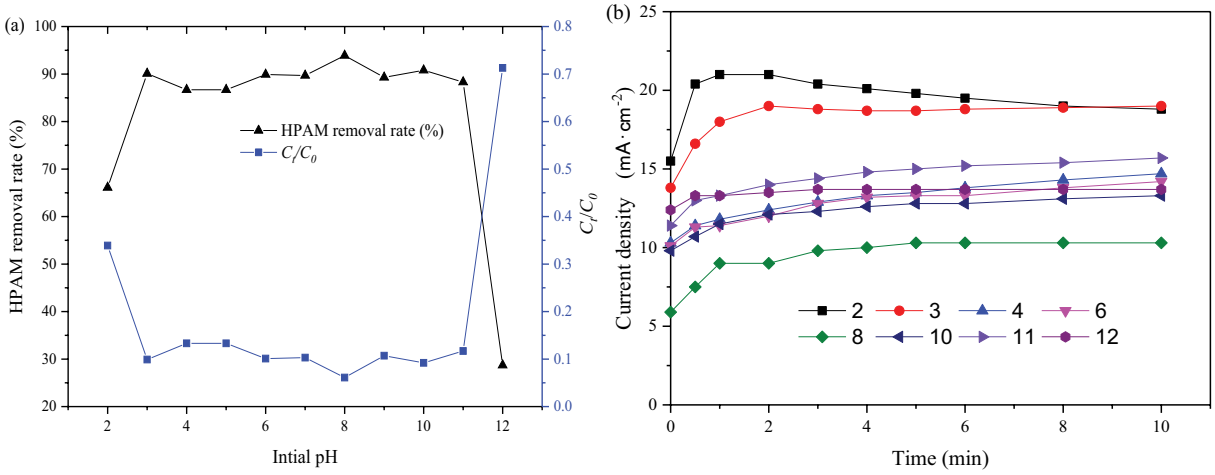

Fig. 6. Effect of the initial pH on the HPAM removal rate for a reaction time of 10 min (a), and the corresponding variation of the current density (b) at an iron electrode (constant voltage: 5 V, temperature: 25°C, electrode distance: 2 cm, reaction time: 10 min).

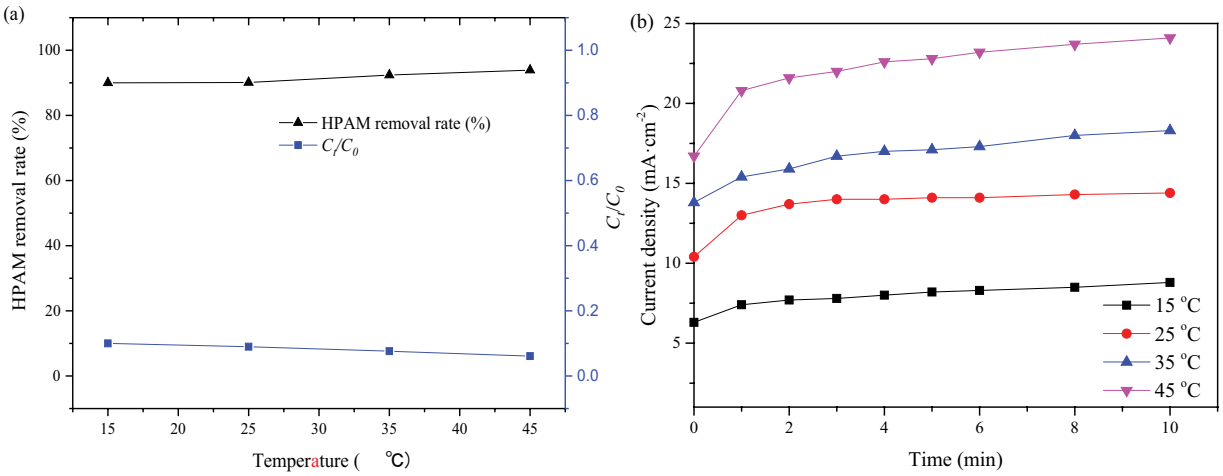

Fig. 7. Effect of temperature on the HPAM removal rate for a reaction time of 10 min (a), and the corresponding variations in the current density (b) at an iron electrode (constant voltage: 5 V, initial pH: 8, electrode distance: 2 cm, reaction time: 10 min).

Table 2
Design matrix of coded units and experimental responses

Test	X_1	X_2	X_3	HPAM removal rate (%)
1	0	1	1	75.5
2	–1	–1	0	8
3	1	0	–1	75.1
4	–1	0	1	9.9
5	0	1	–1	30.7
6	1	0	1	90
7	0	0	0	86.1
8	0	0	0	89.3
9	1	1	0	56.1
10	0	0	0	88.9
11	0	0	0	86.5
12	–1	0	–1	1
13	0	0	0	80.3
14	1	–1	0	89.9
15	0	–1	–1	84
16	–1	1	0	6
17	0	–1	1	85

the p values of less than 0.05 indicated that x_1, x_2, x_3, x_4, x_1x_2, x_2x_3, x_{12}, and x_{22} were very significant. The results show that during the electrochemical treatment of HPAM-containing wastewater, the interactions between the voltage and pH and between the pH and reaction time were obvious; the mismatch was 5.50, and the F value was 0.0665, indicating that there was no significant relationship between the errors. The correlation coefficient (R^2) and standard error can generally be used to investigate the fit of a regression model. Because the R^2 value (0.9863) was very close to 1, this model could be used to predict the degradation rate of HPAM.

The p value for the lack of fit was 0.0665; as this value was higher than 0.05, it indicated that the miscalculation was not significant. The "predicted R-squared" value (0.8195) was close to the "adjusted R-squared" value (0.9687), and the "adequate precision" was 20.356, indicating that the model could reflect changes in the response value well.

The experimental and predicted values were also compared, as shown in Fig. 8. The predicted values were almost same to the actual degradation rates, indicating that the regression function could be used to predict the polymer degradation rates. The maximum residual of less than 3% (Fig. 9) indicated that the predicted polymer degradation rates were well-correlated with the experimental values.

3.8.2. Effects of the individual parameters

In order to provide a clearer interpretation of the effects of the independent variables, Pareto analysis, which is a presentative method and is based on Eq. (12), was used. The Pareto graph is illustrated in Fig. 10 [36]:

$$P_i = \left(\frac{b_i^2}{\sum b_i^2}\right) \times 100 \quad (i \neq 0) \tag{12}$$

Fig. 10 indicates the most important factors were voltage and voltage × voltage, which accounted for 41.09% and 40.52% of the effect, respectively. This is reasonable, as a higher voltage should lead to the production of more $Fe(OH)_3$ and other strongly oxidizing substances. However, the interaction effects of the other parameters were not significant.

3.8.3. Interactions among the variables

The relationships between the response value and the independent variables can be evaluated using response surfaces and contour maps. These plots can be used to find the optimal process parameters and determine the interactions between the parameters. The dot at the center of the contour line is the response surface, and the shape of the contour line indicates the interaction between the two factors; an oval shape represents a significant interaction, while a circular shape represents an insignificant interaction. The slope of

Table 3
ANOVA values of the obtained experimental responses

Source	Estimated coefficient	Degrees of freedom	Sum of squares	Mean square	*F* value	*p* value	Remarks
Intercept/model	86.22	9	19,140.99	2,126.78	56.04	0.0001	Significant
x_1	35.77	1	10,235.73	10,235.73	269.70	0.0001	Significant
x_2	–12.32	1	1,214.43	1,214.43	32.00	0.0008	Significant
x_3	8.70	1	605.35	605.35	15.95	0.0052	Significant
x_1x_2	–7.94	1	252.29	252.29	6.65	0.0366	Significant
x_1x_3	1.50	1	9.03	9.03	0.24	0.6406	Not significant
x_2x_3	10.95	1	479.61	479.61	12.64	0.0093	Significant
x_1^2	–35.52	1	5,311.66	5,311.66	139.96	0.0001	Significant
x_2^2	–10.72	1	483.45	483.45	12.74	0.0091	Significant
x_3^2	–6.70	1	189.27	189.27	4.99	0.0607	Not Significant
Residual		7	265.67	265.67			
Lack of fit		3	213.86	213.86	5.50	0.0665	Not Significant
Pure error		4	51.81	51.81			

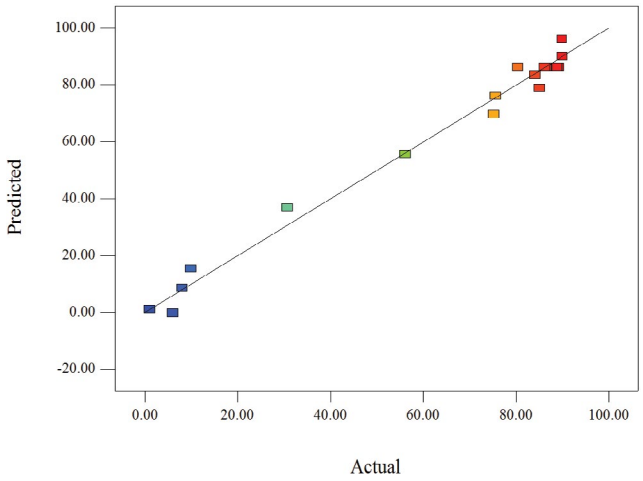

Fig. 8. Predicted vs. actual values for the HPAM removal rate.

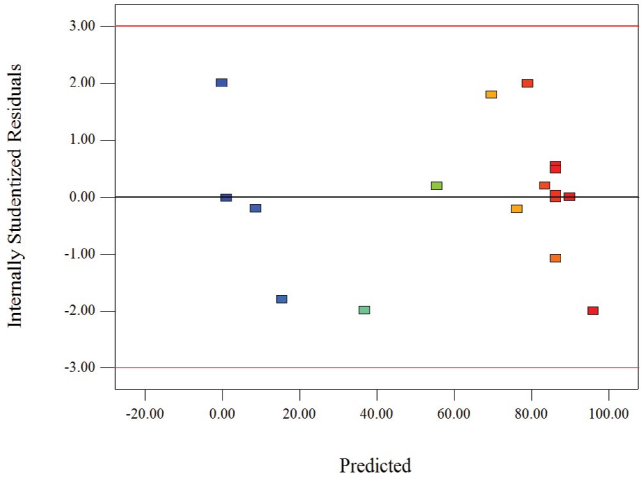

Fig. 9. Internally studentized residuals vs. predicted values plot for the HPAM removal rate.

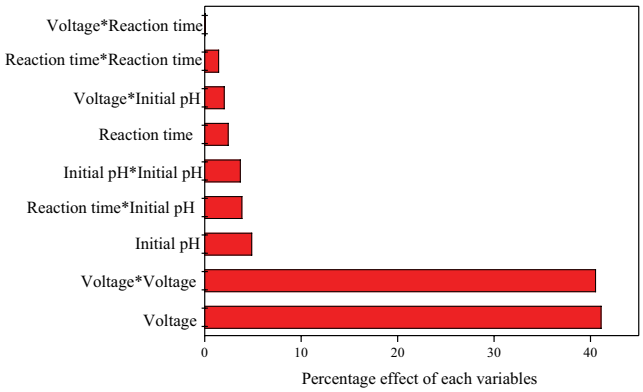

Fig. 10. Pareto chart of the effect of each variable.

the curved surface in the three-dimensional (3D) diagram indicates the degree of influence of the two factors on the response value. Greater inclination (i.e., a steeper slope) indicates more significant influence. In addition, a preliminary determination can be made from the color of the 3D image; as the change increases sharply, the color is deeper.

Fig. 11 shows the two-dimensional (2D) profile and 3D response surface plot of the initial pH–voltage interaction. The HPAM removal rate first increases and then decreases as the initial pH increases, with a maximum at an initial pH of 8, because $Fe(OH)_3$ flocs are more abundant under neutral conditions. The peracid and alkali species change the floc morphology and affect the HPAM removal efficiency [37]. The HPAM removal rate increases with increasing voltage, indicating that the voltage has a greater impact on the experimental result. In the experiments, one factor was maintained at the intermediate level while the other two factors were varied. When the reaction time was increased to 10 min and the voltage was maintained at 1 V, the removal rate of HPAM at pH 4–12 remained relatively constant, changing only from 8% to 6%. However, when the reaction time and pH were maintained at 10 min and 4, respectively,

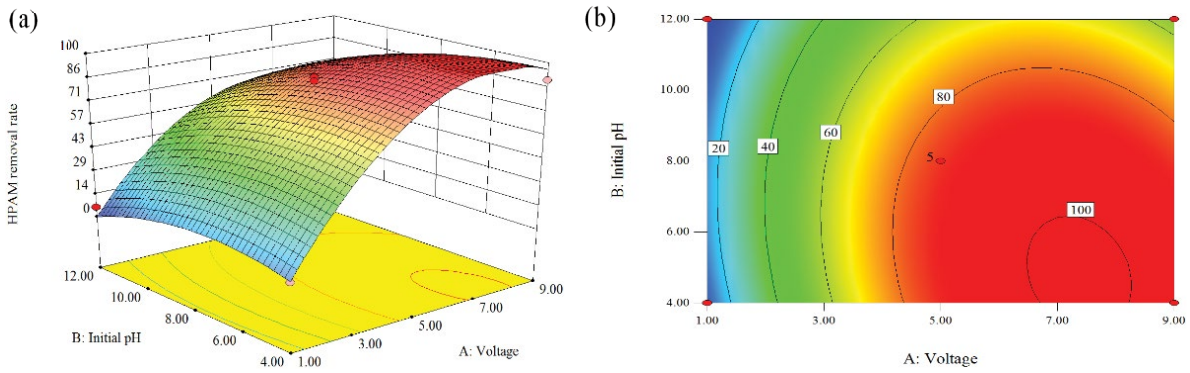

Fig. 11. 3D response surface plot (a) and 2D profile (b) of the effect of the initial pH and the voltage on the HPAM removal rate.

and the voltage was increased from 1 to 9 V, the HPAM removal rate increased from 8% to 89.9%. These results demonstrated that the voltage played a more important role than the initial pH in the experiment. This may be related to that fact that increasing the voltage generates large amounts of Fe^{2+} and OH^- in the reaction system, which can increase the number of flocs and thus improve the HPAM removal rate [38].

Fig. 12 shows that at a voltage of 5 V and an initial pH of 12, the HPAM removal rate increased from 30.7% to 75.5% as the reaction time was increased from 5 to 15 min. The HPAM removal rate was also investigated between pH 12 and 4 at a voltage of 5 V and a reaction time of 15 min. The resulting increase in the removal rate (from 75.5% to 85.0%) was small, indicating that the reaction time was the more dominant of these two factors. As the reaction time was increased, the quantity of $Fe(OH)_2/Fe(OH)_3$ flocs in the reaction system increased, favoring the degradation of HPAM.

3.8.4. Confirmation and validation

Analysis of the surfaces representing the above factors shows that the optimal conditions obtained by the RSM simulation are a voltage of 7.6 V (the current density increased from 19.2 mA cm^{-2} at the beginning to 26.8 mA cm^{-2} at a reaction time of 10.5 min), a pH of 4.7, and a reaction time of 10.5 min. The other conditions were kept constant, with an electrode distance of 2 cm and a temperature of 25°C. The 95% confidence interval of the HPAM removal efficiency was 94.3%–100% for the predicted value. The HPAM removal rate obtained in a verification experiment under these conditions was 98.4%, which was within the confidence interval of the predicted values, indicating a good fit between the experimental results and the predicted value.

3.9. HPAM degradation process

To explore the HPAM degradation pathway, the FT-IR spectra of different samples were obtained, as shown in Fig. 13. The black solid line represents the IR absorption spectrum of solid $Fe(OH)_3$ powder, the blue dot-dash patterned line shows the FT-IR spectrum of the solid powder after EC, and the red dashed line shows the FT-IR spectrum of the HPAM powder. A comparison of the three spectra reveals that after the EC reaction, the characteristic peaks of HPAM at 3,346; 1,662; 1,564; 1,406; and 622 cm^{-1} clearly appeared in the spectrum of the product. These peaks were attributed to –OH stretching, $–NH_2$ stretching, CN stretching, and NH_2 out-of-plane bending, respectively. Thus, it can be inferred that HPAM was present in the $Fe(OH)_3$ colloid flocs, and that the flocs produced by EC obviously adsorbed HPAM.

In addition, a peak corresponding to –O– (1,138 cm^{-1}) was also observed in the IR spectrum, indicating that an intermediate product containing an ether bond was produced during electrochemical degradation. A trace amount of ammonia

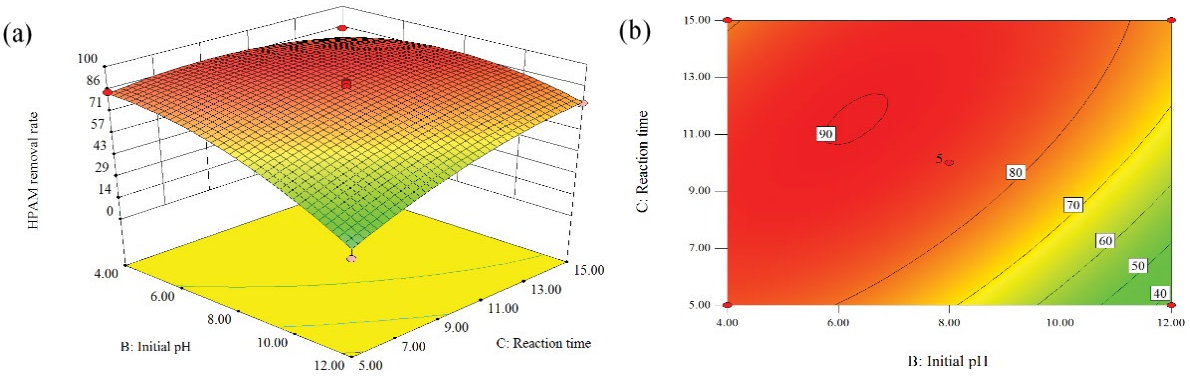

Fig. 12. 3D response surface plot (a) and 2D profile (b) of the effects of the initial pH and the reaction time on the HPAM removal rate.

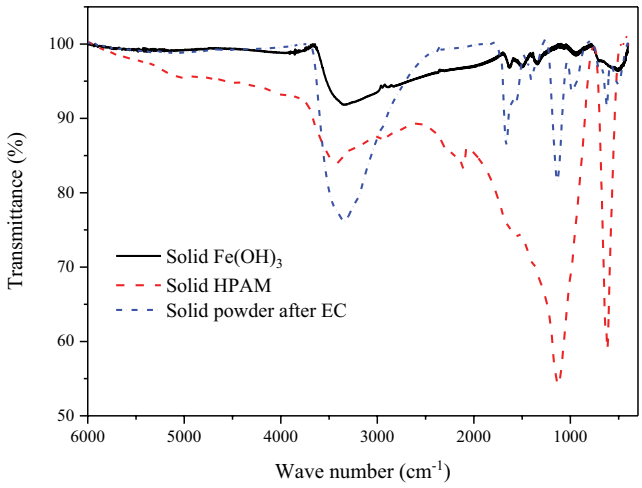

Fig. 13. FT-IR analysis of solid $Fe(OH)_3$, solid HPAM, and the solid powder collected after EC (constant voltage: 7.6 V (current density increased from 19.2 to 29.5 mA cm^{-2} over 15 min of reaction), initial pH: 4.7, reaction time: 10.5 min, electrode distance: 2 cm, temperature: 25°C).

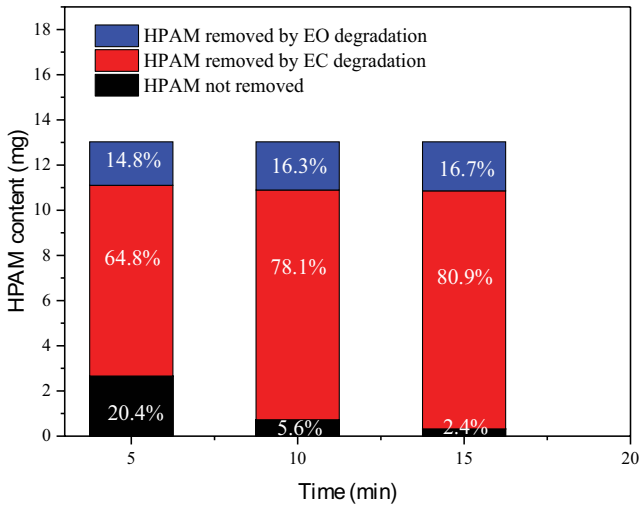

Fig. 14. Percentage of HPAM removed by different methods (constant voltage: 7.6 V (current density increased from 19.2 to 29.5 mA cm^{-2} over 15 min of reaction), initial pH: 4.7, reaction time: 5, 10.5, or 15 min, electrode distance: 2 cm, temperature: 25°C).

(0.2 mg L^{-1}) was detected in the solution after the EC reaction, possibly due to the oxidation of the amino moiety in HPAM to ammonia. This indicated that HPAM was removed by the combined action of EC and EO.

To explore the contributions of EC and EO to HPAM removal, the HPAM contents of the solution and the $Fe(OH)_3$ colloid were measured after a reaction time of 10.5 min. As shown in Fig. 14, the amount of HPAM in the solution before the reaction was determined to be 13.03 mg. At the end of the reaction, the amount of HPAM in the solution was 0.725 mg, and the HPAM removal rate was 94.4%. After the reaction, the flocs were dissolved in acid, and the HPAM content was determined to be 10.17 mg. Therefore, the HPAM removal rate via EC was 83%, and the contribution of EO reduction was determined to be 17%.

3.10. Energy cost

Determination of the energy cost is a necessary process in the development of electrochemical methods. The energy cost can be determined using Eq. (13) below:

$$\text{Electrical energy consumption (EEC)} = \frac{UIt}{V} \quad (13)$$

where U, I, t are the voltage (V), current (A), and electrolysis time (h), respectively; and V is the volume of the sample (m^3). Under the optimal conditions, the electrical energy consumption was 4.63 kwh m^{-3}. The electrical energy consumption per kg of HPAM removed was 23.15 kwh kg^{-1}.

4. Conclusions

In this study, the iron electrode showed the highest HPAM removal rate among the three electrodes investigated, and single-factor experiments were performed to determine the influence of various factors on HPAM degradation. The voltage, initial pH, and reaction time were selected as the three most influential factors and subsequently optimized by RSM using the BBD method. ANOVA showed that all three factors had significant effects, and their degree of influence followed the order voltage > initial pH > reaction time. The optimal conditions for HPAM degradation via EC were a voltage of 7.6 V, pH of 4.7, and reaction time of 10.5 min; under these conditions, an HPAM removal rate of 98.4% was achieved. The experimental value was in good agreement with the predicted value, indicating that this model effectively optimized the operating parameters for the electrochemical degradation of HPAM.

The three factors were found to greatly influence each other in the electrochemical reaction. As voltage was the most important factor, HPAM can be removed efficiently by increasing the voltage. In addition, the initial pH strongly affects the outcome of the experiment, and the HPAM removal improved under weakly acid conditions. An analysis of the experimental products provided insight into the HPAM degradation process. The results of this study should lay a foundation for future work.

Acknowledgments

This work was supported by the National Natural Science Foundation of China (Grant No. 21677018), the Joint Fund of the Beijing Natural Science Foundation and Beijing Municipal Education Commission (Grant No. KZ201810017024), and the Open Project Program of the State Key Laboratory of Petroleum Pollution Control (Grant No. PPC2017006), CNPC Research Institute of Safety and Environmental Technology.

References

[1] S. Fang, M. Duan, W. Long, Y. Ma, H. Wang, J. Zhang, Treatment of produced liquid from polymer flooding by using cationic surfactant, Sep. Sci. Technol., 49 (2014) 432–437.

[2] Y. Pi, Z. Zheng, M. Bao, Y. Li, Y. Zhou, G. Sang, Treatment of partially hydrolyzed polyacrylamide wastewater by combined Fenton oxidation and anaerobic biological processes, Chem. Eng. J., 273 (2015) 1–6.
[3] M. Zhu, J. Yao, W. Wang, X. Yin, W. Chen, X. Wu, Using response surface methodology to evaluate electrocoagulation in the pretreatment of produced water from polymer-flooding well of Dagang Oilfield with bipolar aluminum electrodes, Desal. Wat. Treat., 57 (2016) 15314–15325.
[4] M. Duan, Y. Ma, S. Fang, P. Shi, J. Zhang, B. Jing, Treatment of wastewater produced from polymer flooding using poly oxyalkylated polyethyleneimine, Sep. Purif. Technol., 133 (2014) 160–167.
[5] J. Liu, J. Ren, R. Xu, B. Yu, J. Wang, Biodegradation of partially hydrolyzed polyacrylamide by immobilized bacteria isolated from HPAM-containing wastewater, Environ. Prog. Sustain., 35 (2016) 1344–1352.
[6] E. Karamati-Niaragh, M.R.A. Moghaddam, M.M. Emamjomeh, E. Nazlabadi, Evaluation of direct and alternating current on nitrate removal using a continuous electrocoagulation process: economical and environmental approaches through RSM, J. Environ. Manage., 230 (2019) 245–254.
[7] F. Hussin, F. Abnisa, G. Issabayeva, M.K. Aroua, Removal of lead by solar-photovoltaic electrocoagulation using novel perforated zinc electrode, J. Clean. Prod., 147 (2017) 206–216.
[8] S. Elabbas, N. Ouazzani, L. Mandi, F. Berrekhis, M. Perdicakis, S. Pontvianne, M.N. Pons, F. Lapicque, J.P. Leclerc, Treatment of highly concentrated tannery wastewater using electrocoagulation: Influence of the quality of aluminium used for the electrode, J. Hazard. Mater., 319 (2016) 69–77.
[9] H.K. Hansen, S.F. Peña, C. Gutiérrez, A. Lazo, P. Lazo, L.M. Ottosen, Selenium removal from petroleum refinery wastewater using an electrocoagulation technique, J. Hazard. Mater., 364 (2019) 78–81.
[10] H. Zazou, H. Afanga, S. Akhouairi, H. Ouchtak, A.A. Addi, R.A. Akbour, A. Assabbane, J. Douch, A. Elmchaouri, J. Duplay, A. Jada, M. Hamdani, Treatment of textile industry wastewater by electrocoagulation coupled with electrochemical advanced oxidation process, J. Water. Process. Eng., 28 (2019) 214–221.
[11] K.G. Ravindra, C.C. Mahesh, Advanced Nanomaterials for Wastewater Remediation, CRC Press, Boca Raton, 2016, pp. 62–101.
[12] A. Mirza, A. King, C. Troakes, C. Exley, Aluminium in brain tissue in familial Alzheimer's disease, J. Trace Elem. Med Biol., 40 (2017) 30–36.
[13] M. Chafi, B. Gourich, A.H. Essadki, C. Vial, A. Fabregat, Comparison of electrocoagulation using iron and aluminium electrodes with chemical coagulation for the removal of a highly soluble acid dye, Desalination, 281 (2011) 285–292.
[14] I. Zongo, A.H. Maiga, J. Wéthé, G. Valentin, J.-P. Leclerc, G. Paternotte, F. Lapicque, Electrocoagulation for the treatment of textile wastewaters with Al or Fe electrodes: compared variations of COD levels, turbidity and absorbance, J. Hazard. Mater., 169 (2009) 70–76.
[15] M. Ahmadi, F. Ghanbari, Optimizing COD removal from greywater by photoelectro-persulfate process using Box-Behnken design: assessment of effluent quality and electrical energy consumption, Environ. Sci. Pollut. Res., 23 (2016) 19350–19361.
[16] F. Zaviska, P. Drogui, J.-F. Blais, G. Mercier, Electrochemical treatment of bisphenol-A using response surface methodology, J. Appl. Electrochem., 42 (2012) 95–109.
[17] J.E. Silveira, J.A. Zazo, G. Pliego, E.D. Bidoia, P.B. Moraes, Electrochemical oxidation of landfill leachate in a flow reactor: optimization using response surface methodology, Environ. Sci. Pollut. Res., 22 (2015) 5831–5841.
[18] M. Zhu, J. Yao, Z. Qin, L. Lian, C. Zhang, Response surface methodology approach for the optimisation of adsorption of hydrolysed polyacrylamide from polymer-flooding wastewater onto steel slag: a good option of waste mitigation, Water Sci. Technol., 76 (2017) 776–784.
[19] M. Ahmadi, F. Ghanbari, S. Madihi-Bidgoli, Photoperoxi-coagulation using activated carbon fiber cathode as an efficient method for benzotriazole removal from aqueous solutions: modeling, optimization and mechanism, J. Photochem. Photobiol. A, 322 (2016) 85–94.
[20] Y.R. Wang, L. Wang, Study on the treatment of anthraquinone dye wastewater with different electrode material, J. Wuhan Inst. Technol., 31 (2009) 31–34 (In Chinese).
[21] H.L. Wang, J.Y. Cui, W.F. Jiang, Synthesis, characterization and flocculation activity of novel Fe(OH)(3)-polyacrylamide hybrid polymer, Mater. Chem. Phys., 130 (2011) 993–999.
[22] V. Khandegar, A.K. Saroha, Electrocoagulation for the treatment of textile industry effluent – a review, J. Environ. Manage., 128 (2013) 949–963.
[23] M. Yoosefian, S. Ahmadzadeh, M. Aghasi, M. Dolatabadi, Optimization of electrocoagulation process for efficient removal of ciprofloxacin antibiotic using iron electrode; kinetic and isotherm studies of adsorption, J. Mol. Liq., 225 (2017) 544–553.
[24] M. Elazzouzi, K. Haboubi, M.S. Elyoubi, Electrocoagulation flocculation as a low-cost process for pollutants removal from urban wastewater, Chem. Eng. Res. Des., 117 (2017) 614–626.
[25] A.K. Verma, Treatment of textile wastewaters by electrocoagulation employing Fe-Al composite electrode, J. Water. Process. Eng., 20 (2017) 168–172.
[26] P. Aswathy, R. Gandhimathi, S.T. Ramesh, P.V. Nidheesh, Removal of organics from bilge water by batch electrocoagulation process, Sep. Purif. Technol., 159 (2016) 108–115.
[27] S. Bayar, Y.S. Yildiz, A.E. Yilmaz, S. Irdemez, The effect of stirring speed and current density on removal efficiency of poultry slaughterhouse wastewater by electrocoagulation method, Desalination, 280 (2011) 103–107.
[28] M. Kobya, E. Demirbas, Evaluations of operating parameters on treatment of can manufacturing wastewater by electrocoagulation, J. Water Process. Eng., 8 (2015) 64–74.
[29] L. Xu, G. Cao, X. Xu, C. He, Y. Wang, Q. Huang, M. Yang, Sulfite assisted rotating disc electrocoagulation on cadmium removal: parameter optimization and response surface methodology, Sep. Purif. Technol., 195 (2018) 121–129.
[30] P. Song, Z. Yang, G. Zeng, X. Yang, H. Xu, L. Wang, R. Xu, W. Xiong, K. Ahmad, Electrocoagulation treatment of arsenic in wastewaters: a comprehensive review, Chem. Eng. J., 317 (2017) 707–725.
[31] X. Chen, P. Ren, T. Li, J.P. Trembly, X. Liu, Zinc removal from model wastewater by electrocoagulation: processing, kinetics and mechanism, Chem. Eng. J., 349 (2018) 358–367.
[32] Z.B. Gönder, G. Balcıoğlu, I. Vergili, Y. Kaya, Electrochemical treatment of carwash wastewater using Fe and Al electrode: techno-economic analysis and sludge characterization, J. Environ. Manage., 200 (2017) 380.
[33] A. Attour, M. Touati, M. Tlili, M. Ben Amor, F. Lapicque, J.P. Leclerc, Influence of operating parameters on phosphate removal from water by electrocoagulation using aluminum electrodes, Sep. Purif. Technol., 123 (2014) 124–129.
[34] D.G. Bassyouni, H.A. Hamad, E.S.Z. El-Ashtoukhy, N.K. Amin, M.M.A. El-Latif, Comparative performance of anodic oxidation and electrocoagulation as clean processes for electrocatalytic degradation of diazo dye Acid Brown 14 in aqueous medium, J. Hazard. Mater., 335 (2017) 178–187.
[35] L. Yue, L. Wang, F. Shi, J. Guo, J. Yang, J. Lian, X. Luo, Application of response surface methodology to the decolorization by the electrochemical process using $FePMo_{12}O_{40}$ catalyst, J. Ind. Eng. Chem., 21 (2015) 971–979.
[36] M. Moradi, F. Ghanbari, E.M. Tabrizi, Removal of acid yellow 36 using Box-Behnken designed photoelectro-Fenton: a study on removal mechanisms, Toxicol. Environ. Chem., 97 (2015) 700–709.
[37] M.K.N. Mahmad, M.A.Z.M.R. Rozainy, I. Abustan, N. Baharun, Electrocoagulation process by using aluminium and stainless steel electrodes to treat total chromium, colour and turbidity, Procedia Chem., 19 (2016) 681–686.
[38] Y.A. Ouaissa, M. Chabani, A. Amrane, A. Bensmaili, Removal of tetracycline by electrocoagulation: kinetic and isotherm modeling through adsorption, J. Environ. Chem. Eng., 2 (2014) 177–184.